COMPARISON OF FOUR FILTERING OPTIONS FOR A RADAR TRACKING PROBLEM

John A. Lawton, Robert J. Jesionowski
Naval Surface Warfare Center, Dahlgren Division, Dahlgren, Virginia
and
Paul Zarchan
Charles Stark Draper Lab, Cambridge, Massachusetts

Abstract

Four different filtering options are considered for the problem of tracking an exoatmospheric ballistic target with no maneuvers. The four filters are an alpha-beta filter, an augmented alpha-beta filter, a decoupled Kalman filter, and a fully-coupled extended Kalman filter. These filters are listed in the order of increasing computational complexity. All of the filters can track the target with some degree of accuracy. While the pure alpha-beta filter appreciably lags the other filters in performance for this problem, its augmented version is very competitive with the extended Kalman filter under benign conditions. Perhaps the most surprising result is that under all conditions examined, the decoupled (linear) Kalman filter, which is at least an order of magnitude less computationally complex, performs nearly identical to the coupled, extended Kalman filter.

Introduction

Kalman filtering became immediately popular when it was first introduced in the 1960's, even though the initial journal papers were incomprehensible to many experienced engineers[1,2]. This new filtering technique was popular in the academic community because it could be shown that the Kalman filter was optimal in some sense, and, in addition, Kalman filtering was also popular in industry because its form was ideal for implementation on a digital computer. After three decades, applications of Kalman filtering have proliferated to the point where today many younger engineers do not even know the existence of other types of filters[3,4].

In some applications today, because of the availability of computational plenty, the standard approach is often to implement a fully coupled Kalman filter without consideration of simpler implementations or even other types of filters. In this paper, we will consider several types of filters, ranging from an alpha-beta filter (non-Kalman) to a fully coupled Kalman filter, for an application in which a ship radar is tracking an exoatmospheric target. It is assumed that the target is not maneuvering, and that the filter must estimate the position and velocity of the target based on range and angle measurements.

Four different types of filters will be compared in terms of the quality of their estimates, and in terms of their computational complexity. The filters will be first compared under benign conditions in which all the measurement data is available, and then compared under conditions in which large portions of the measurements are lost.

Contrary to popular opinion, it will be shown that under benign conditions for this exoatmospheric tracking problem all filters yield approximately the same performance. Under these circumstances an alpha-beta filter can yield excellent performance at orders of magnitude less computational complexity than a fully coupled Kalman filter. Under conditions in which there are large blackout periods, it will be shown that a decoupled Kalman filter can yield performance similar to that of a fully coupled filter at an order of magnitude less computational complexity.

Filter Formulations

Four different filter designs will be presented. The first three are all decoupled filters, meaning that the whole six-dimensional state is broken up into three two-dimensional states, which are updated in the filter equations independently. Each two-dimensional state is comprised of position and velocity along one of

the Earth-fixed Cartesian coordinate directions in an East-North-Up (ENU) coordinate system centered at the sensor.

The first filter is an alpha-beta filter, which can be derived as a steady state two-dimensional Kalman filter[5]. Since alpha-beta filters have constant gains (for a given sensor to target range), and it is well known the Kalman filter's typically steadily decreasing gain is optimal (for a linear problem), a simple design is to tack onto the alpha-beta filter a "growing-memory" filter during the settling portions. That is, a growing-memory filter (which is actually a zero-process-noise Kalman filter) is used during the initial portions of the observation of the target[6], and the alpha-beta filter is used after the initial settling is finished. This hybrid filter will be called the growing-memory/alpha-beta (GMAB) filter. The third filter is just a decoupled Kalman filter -- that is, it is three independent two-dimensional Kalman filters, one for each coordinate direction.

The fourth filter is a multiple coordinate system, fully coupled extended Kalman filter. The state and covariance propagations are done in an Earth-centered inertial (ECI) coordinate system, and the measurement updates are done in a range/direction-cosine coordinate system. The dynamics model is Keplerian motion.

The Decoupled Filters

All three of the decoupled filters are designed with a nominally zero acceleration model. Hence, each two-dimensional state x, with the first component of x being position and the second component being velocity, is assumed to have the following discrete-time dynamics, propagating the state from the time of the kth measurement, t_k, to that of the $(k+1)$st:

$$x_{k+1} = \Phi(k+1,k)\, x_k + \omega_k \qquad (1)$$

where

$$\Phi(k+1,k) \triangleq \begin{bmatrix} 1 & T \\ 0 & 1 \end{bmatrix},$$

$$T \triangleq t_{k+1} - t_k \ ,$$

and ω_k is the process noise, with

$$\mathrm{E}(\omega_k) = 0\,, \text{ and } \mathrm{E}(\omega_k\, \omega_k^T) = Q \ .$$

Since the position vector is measured by a radar, the scalar measurement is

$$z = H\, x + \nu \ ,$$

where

$$H = [\,1 \quad 0\,],$$

and ν is a white noise disturbance random variable, with

$$\mathrm{E}(\nu) = 0\,, \text{ and } \mathrm{E}(\nu^2) = R = \sigma_m^2 \ .$$

For all of the decoupled filters, the measurement standard deviation, σ_m, will be estimated by

$$\sigma_m = \overline{\rho} \cdot \sigma_a \,,$$

where $\overline{\rho}$ is the current estimated range to the target, and σ_a is the angular error of the radar.

All of the decoupled filters used for this study have process noise predicated upon a piecewise constant white acceleration model[7]. Hence,

$$Q = \begin{bmatrix} T^4/4 & T^3/2 \\ T^3/2 & T^2 \end{bmatrix} \cdot \epsilon^2, \qquad (2)$$

where in practice ϵ is a parameter used to tune the filter.

While the filter theory has its dynamics predicated on Eq. (1), the decoupled filters actually use a piecewise constant acceleration model for the propagation of the state vector from the kth measurement to the $(k+1)$st measurement. The total acceleration vector, denoted by $\vec{a} = [\,a_e \quad a_n \quad a_u\,]^T$ (e, n, and u represent East, North, and up, respectively), is the sum of the inverse-square gravity acceleration, Coriolis acceleration, and centripetal acceleration, computed at time t_k. So, with $\overline{x}_k$ representing the filter's estimate of the state at time t_k *before measurement* (for any of the three coordinate directions), and $\widehat{x}_k$ representing the estimate at time t_k *after measurement*,

$$\overline{x}_{k+1} = \Phi(k+1,k)\, \widehat{x}_k + \begin{bmatrix} \frac{1}{2} a_i T^2 \\ a_i T \end{bmatrix} \qquad (3)$$

where a_i (with $i \in \{e, n, u\}$) is the component of acceleration in this particular direction. $\vec{a}$ is computed by

$$\vec{a} = \vec{g} + \vec{c} + \vec{p} \ ,$$

where

$$\vec{g} = -\frac{\mu}{R^3} \vec{R} \ ,$$

$$\vec{c} = -2\vec{\omega} \times \vec{v} \ ,$$

and

$$\vec{p} = -\vec{\omega} \times (\vec{\omega} \times \vec{r}) \ ,$$

with $\vec{\mathrm{r}} = [\, r_e \quad r_n \quad r_u \,]^T$ and $\vec{v} = [\, v_e \quad v_n \quad v_u \,]^T$ being the position and velocity vectors in ENU at time t_k,

$$\vec{R} = \vec{r} + \begin{bmatrix} 0 \\ 0 \\ R_{\mathrm{E}} \end{bmatrix} \ ,$$

and $\vec{\omega}$ is the angular motion of the Earth in ENU. Denoting the latitude of the sensor by ϕ, and the rotation rate of the Earth by ω_{E},

$$\vec{\omega} = \omega_{\mathrm{E}} \begin{bmatrix} 0 \\ \cos\phi \\ \sin\phi \end{bmatrix} \ ,$$

which yields

$$\vec{c} = \begin{bmatrix} -2\omega_{\mathrm{E}}(v_u \cos\phi - v_n \sin\phi) \\ -2\omega_{\mathrm{E}} v_e \sin\phi \\ 2\omega_{\mathrm{E}} v_e \cos\phi \end{bmatrix}$$

and

$$\vec{p} = \begin{bmatrix} \omega_{\mathrm{E}}^2 r_e \\ -\omega_{\mathrm{E}}^2 (r_u \cos\phi - r_n \sin\phi)\sin\phi \\ \omega_{\mathrm{E}}^2 (r_u \cos\phi - r_n \sin\phi)\cos\phi \end{bmatrix} \ .$$

The components of $\vec{c}$ and $\vec{p}$ are used in Eq. (3) to propagate to the next measurement time.

The only difference between the three decoupled filters in this study is the choice of the values used in the 2×1 gain matrix K, for use in the usual update equation:

$$\hat{x} = \bar{x} + K\,(z - H\bar{x}) \,. \qquad (4)$$

Alpha-Beta Filter

The name of the alpha-beta filter comes from the parameters alpha and beta (α and β), which are defined such that the gain matrix is

$$K = \begin{bmatrix} \alpha \\ \beta/T \end{bmatrix} .$$

Defining the so-called maneuvering index

$$\lambda = \frac{\epsilon \cdot T^2}{\bar{\rho} \cdot \sigma_a} \ ,$$

α and β can be computed with[5]

$$\alpha = -\frac{1}{8}\left(\lambda^2 + 8\lambda - (\lambda+4)\sqrt{\lambda^2+8\lambda}\right) \qquad (5)$$

and

$$\beta = \frac{1}{4}\left(\lambda^2 + 4\lambda - \lambda\sqrt{\lambda^2+8\lambda}\right) \ .$$

Hybrid Growing-Memory/Alpha-Beta Filter

The alpha-beta part of this hybrid filter is the same as described in the previous subsection. Bar-Shalom and Li show that the gains can be expressly written as a function of k, the measurement update number (or time index), for the case of a zero-process-noise Kalman filter (a Kalman filter with $\omega_k = 0$) with the dynamics given in Eq. (1)[6]. The result is

$$K = \begin{bmatrix} \frac{4k+2}{(k+1)(k+2)} \\ \frac{6}{(k+1)(k+2)T} \end{bmatrix} \ . \qquad (6)$$

These gains monotonically decrease with time, because the larger amount of data incorporated (or "stored") in the state estimate from past measurements indicates that state needs to be altered less and less based on an individual measurement. That is, the "memory" (or "information") resident in the state estimate is growing -- hence this is also called a growing-memory filter. For small k, these gains are much larger than the alpha-beta gains. Also, for small k, these gains are very similar to Kalman filter gains (with nonzero process noise), because they are more dominated by the large decreases in the state covariance due to additional measurement updates than by the process noise. These gains tend to zero for large k, however, because of the no-noise assumption. Hence, it is advantageous to transition to the steady-state Kalman filter (the alpha-beta filter) for some judiciously chosen value of k. For this study, the simple strategy is used of switching to the alpha-beta filter when the position gain (the 1,1 element of K) from Eq. (6) is smaller than α of Eq. (5).

Decoupled Kalman Filter

The Kalman filter approach is to keep track of an estimate of the state errors in the covariance matrix, P, and the covariance of the so-called "innovation" or "residual," S, then compute the gain as the "ratio" between these two matrices:

$$K = \overline{P} H^T S^{-1} \ . \qquad (7)$$

The innovation is the $(z - H\overline{x})$ term in Eq. (4); $H\overline{x}$ could be labeled $\overline{z}$ since it is the estimate of the measurement before measurement, so the difference is the measurement residual, also called the innovation because it is the mechanism for injecting new information into the state estimate. The covariance of this innovation is

$$S = H\overline{P}H^T + R \ . \qquad (8)$$

The state covariance is propagated between measurements by

$$\overline{P}^{k+1} = \Phi(k+1,k)\widehat{P}^k\Phi^T(k+1,k) + Q \quad (9)$$

and is updated at measurement time by

$$\widehat{P}^{k+1} = \overline{P}^{k+1} - K^{k+1}S^{k+1}\left(K^{k+1}\right)^T. \quad (10)$$

Since P is symmetric, the 2×2 matrix for this problem has only three unique terms. For Eq. (9), these are

$$\overline{P}_{11}^{k+1} = \widehat{P}_{11}^k + 2\widehat{P}_{12}^k T + \widehat{P}_{22}^k T^2 + Q_{11} \ ,$$

$$\overline{P}_{12}^{k+1} = \widehat{P}_{12}^k + \widehat{P}_{22}^k T + Q_{12} \ ,$$

and

$$\overline{P}_{22}^{k+1} = \widehat{P}_{22}^k + Q_{22} \ .$$

The elements of Q come from Eq. (2). The innovation covariance is

$$S^{k+1} = \overline{P}_{22}^{k+1} + R^{k+1} \ .$$

Eq. (10) becomes

$$\widehat{P}_{11}^{k+1} = \frac{\overline{P}_{11}^{k+1}R^{k+1}}{S^{k+1}} \ ,$$

$$\widehat{P}_{12}^{k+1} = \frac{\overline{P}_{12}^{k+1}R^{k+1}}{S^{k+1}} \ ,$$

and

$$\widehat{P}_{22}^{k+1} = \overline{P}_{22}^{k+1} - \frac{\left(\overline{P}_{12}^{k+1}\right)^2}{S^{k+1}} \ .$$

Finally, the Kalman gain, Eq. (7), is

$$K^{k+1} = \begin{bmatrix} \overline{P}_{11}^{k+1}/S^{k+1} \\ \overline{P}_{12}^{k+1}/S^{k+1} \end{bmatrix} \ .$$

Coupled Kalman Filter

The coupled Kalman filter is by far the most complex of the four filters. The 6-dimensional state is

$$x = \begin{bmatrix} \vec{r} \\ \vec{v} \end{bmatrix} \ ,$$

where $\vec{r}$ and $\vec{v}$ are the position and velocity vectors of the target in ECI coordinates. The state is propagated forward in time using analytical Keplerian motion equations, which are the solution to the problem of motion under inverse-square gravity[8]. As for $\Phi(k+1,k)$, it is computed with numerical partial derivatives of the Keplerian solutions of the state:

$$\Phi(k+1,k) = \frac{\partial\, x(t_{k+1})}{\partial\, x(t_k)} \ .$$

The process noise covariance, Q, is the same as Eq. (2), except that each term is multiplied by the 3×3 identity matrix. Given these, Eq. (9) is used to propagate the state covariance forward in time to the next measurement.

In order to effect the measurement update, the state and covariance are transformed from the ECI to the RUV space. The RUV state is defined to be

$$y = \begin{bmatrix} r \\ u \\ v \\ \dot{r} \\ \dot{u} \\ \dot{v} \end{bmatrix} \ ,$$

where r is the range from the sensor to the target, u is the direction cosine of the range vector with respect to the x-axis of the floating frame, and v is the direction cosine with respect to the y-axis of the floating frame. The floating frame is a Cartesian frame defined at each measurement update time, with z pointing toward the estimated position at the update time, x is in the vertical plane (generally "up" -- that is, having a non-negative projection onto any vector which is purely vertical at the sensor), and y is in the horizontal plane. The measurement is taken to be

$$z = \begin{bmatrix} r \\ u \\ v \end{bmatrix} \ ,$$

so that

$$H = [\, I \quad 0 \,] \; .$$

The measurement covariance matrix is approximated well by

$$R = \begin{bmatrix} \sigma_r^2 & 0 & 0 \\ 0 & \sigma_a^2 & 0 \\ 0 & 0 & \sigma_a^2 \end{bmatrix} . \qquad (11)$$

Let $g(x)$ represent the nonlinear transformation from ECI to RUV. Then at update-time index k,

$$\overline{y}_k = g(\overline{x}_k)$$

is the state transformation. To transform the state covariance, first the Jacobian of the transformation is analytically computed at $\overline{x}_k$:

$$J = \left. \frac{\partial\, g(x)}{\partial\, x} \right|_{\overline{x}_k} . \qquad (12)$$

Then, denoting the covariance of y by P_y,

$$\overline{P}_y^k = J\, \overline{P}^k J^T \; .$$

At this point, the state and its covariance are updated in the usual manner in the RUV space. The innovation covariance, Eq. (8), and the Kalman gain, Eq. (7), are computed using R and $\overline{P}_y^k$, whence the state update and the state-covariance update are performed using Eq. (4) and Eq. (10), respectively (with y being used in place of x in Eq. (4)).

The final step is to effect the inverse transformation from the RUV space to the ECI space:

$$\widehat{x}_k = g^{-1}(\widehat{y}_k)$$

and

$$\widehat{P}^k = J^{-1} \widehat{P}_y^k \left(J^{-1}\right)^T$$

(with J having been evaluated again at $\widehat{x}_k$). With this, a full measurement cycle, from propagation to measurement update, is complete.

Filter Initialization

All of the filters are initialized in essentially the same manner. The state is initialized with the position vector equal to the first measurement (or the first measurement transformed to ECI for the coupled Kalman), and the initial velocity is set to zero.

The Kalman filters need their covariances initialized also. For the decoupled Kalman,

$$P_0 = \begin{bmatrix} (\rho\, \sigma_a)^2 & 0 \\ 0 & L \end{bmatrix} ,$$

with L set to 5 km^2/s^2. For the coupled Kalman,

$$P_0 = \begin{bmatrix} J^{-1} R (J^{-1})^T & 0 \\ 0 & L \cdot I \end{bmatrix} ,$$

where I is the 3×3 identity matrix, and R and J are as defined in Eqs. (11) and (12).

Other initialization methods are possible, such as initializing the velocity with the difference between the first two measurements divided by the time between the measurements. It can be shown, however, that this yields significantly degraded performance for the first several measurements for the ballistic missile problem (because excellent upper bounds are known for ballistic missiles, which can be taken advantage of in the covariance initialization)[9]. On the other hand, it can also be shown that after the first few seconds, the differences in the performance of the different initialization methods is totally negligible.

Computational Complexity

The issue of computational complexity is important to this study. The two alpha-beta filters are the least complex by far because, first of all, the computations for the gains are simple. More importantly, the alpha-beta filter gains can be computed via a table look-up, as a function of the maneuvering index. Similarly, the growing memory filter can also be computed via table look-up.

The decoupled Kalman filter is also very competitive in having low complexity. It is propagated with the same equations as the alpha-beta filters, and the whole covariance process and gains calculations for one cycle has only seven additions, one subtraction, eight multiplications, and five divisions. That is hardly a computational burden! In fact, it is even slightly less of a computational load than the alpha-beta filter if the alpha-beta filter were computed on-line as opposed to via table look-up.

The coupled Kalman filter, on the other hand, is full of matrix inversions, matrix multiplications, and, for the specific variety examined here, nonlinear transformations and

trigonometric evaluations. It is quite computationally complex.

Results

The target trajectory used for the numerical results is a 1000 km, minimum energy ballistic missile trajectory created with a rotating earth model, using oblate-earth gravity. The ground track of this trajectory is plotted in Fig. 1, and the ground-range/altitude profile is shown in Fig. 2. The two sensor locations used are also shown, along with vectors to the first detection point on the trajectory from each of these locations.

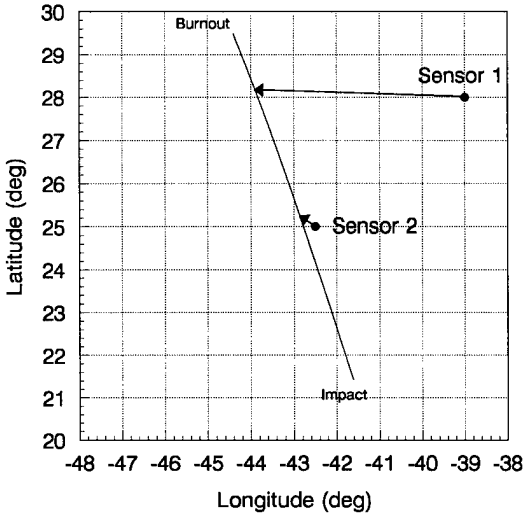

Figure 1. Target and Sensor Geometries.

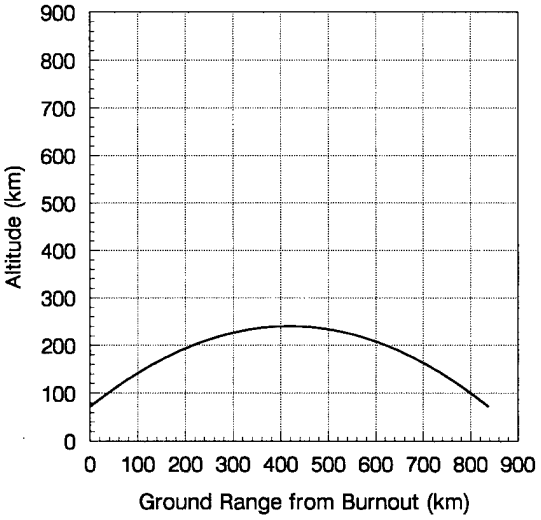

Figure 2. Target Vertical Plane Profile.

For Sensor 1, the detection range is 550 km, the angular error on the radar is 3 mrad, and the range error is 25 m. The measurement rate is one measurement every quarter of a second. Both of the Kalman filters have the process noise parameter $\epsilon = 1\ \mathrm{m/s^2}$, as does the alpha-beta portion of the GMAB filter. Each of the error curves are the RMS values of the true errors from 100 Monte-Carlo realizations.

The first results to be presented are the position and velocity errors of the alpha-beta filter at sensor position 1, for three different levels of ϵ, compared with the coupled Kalman filter, shown in Fig. 3 and Fig. 4. For higher values of the process noise, the alpha-beta filter responds much more rapidly. That is, the errors drop down to near their steady state value more rapidly. The $\epsilon = 100$ m/s case responds almost as rapidly as the coupled Kalman. On the other hand, the lower the value of ϵ is, the lower the steady state errors are. For example, the $\epsilon = 1$ m/s case settles as low as the Kalman, but it requires nearly the whole trajectory to do so. $\epsilon = 10$ m/s is a compromise that yields a reasonable balance between the settling rate and the steady-state error level.

This example demonstrates the general trend of pure alpha-beta filters for ballistic trajectories: you can have fast settling, or low settling, but not both. Of course, the alpha-beta filter will perform better if varying levels of gains are chosen, starting high, and ending low. This, however, is precisely what the GMAB and the Kalman filters are designed to do automatically.

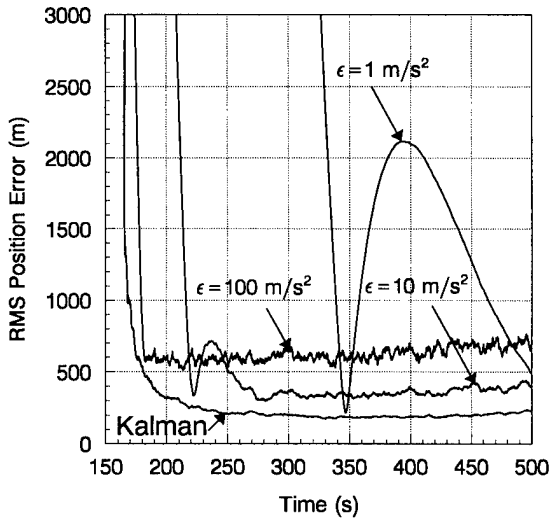

Figure 3. Position Errors for Alpha-Beta Filter.

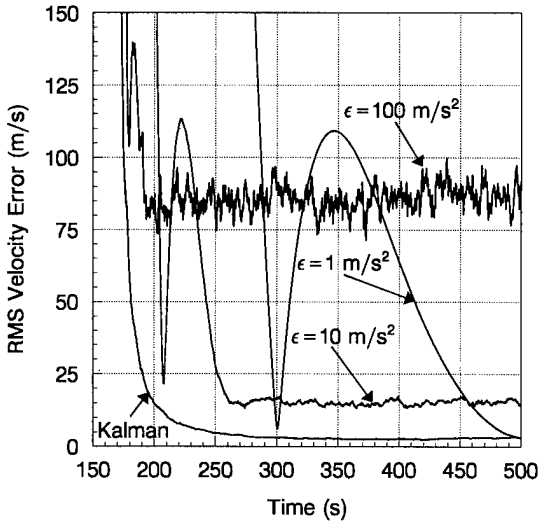

Figure 4. Velocity Errors for the Alpha-Beta Filter.

Fig. 5 and Fig. 6 show the results of the GMAB and the Kalman filters for the same case as presented above. All three of the filters behave nearly the same. In fact, the differences between the GMAB and the decoupled Kalman cannot be discerned on the plots. And both of these decoupled filters behave nearly the same as the fully coupled extended Kalman filter.

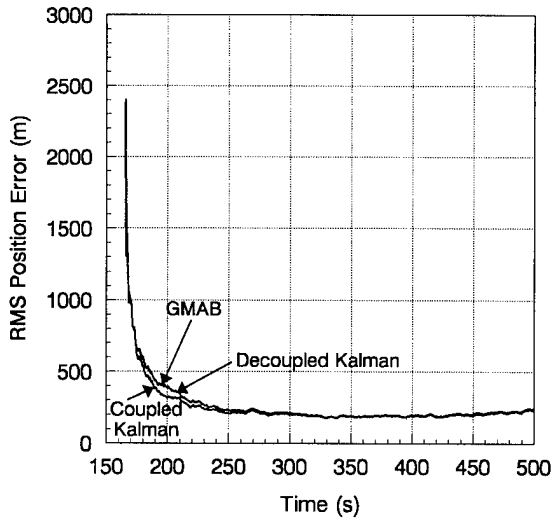

Figure 5. Position Errors for GMAB and Kalman Filters at Sensor Position 1.

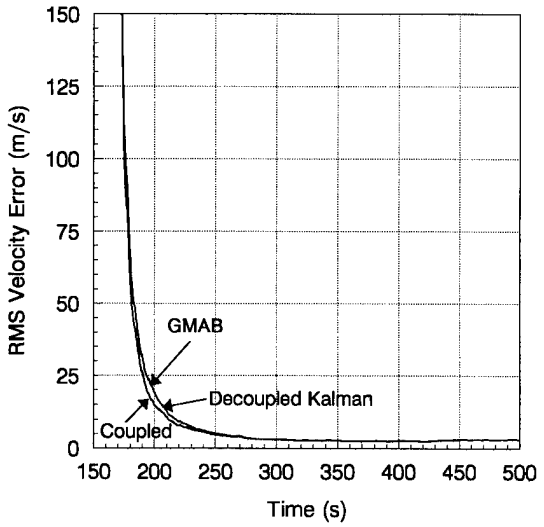

Figure 6. Velocity Errors for GMAB and Kalman Filters at Sensor Position 1.

Next, consider a totally different geometry. At sensor position 2, the detection range is 250 km, so the transverse linear error is smaller for the same 3 mrad angular error, and the direction is nearly vertical (since the apogee height of the trajectory is nearly 250 km), as opposed to the nearly horizontal position vector of the Sensor 1 case. In other words, the geometry is quite different from the first case. The relative results between these three variable-gain filters, however, is the same, as can be seen in Fig. 7. (For the sake of brevity, only the velocity curves will be shown for most of the subsequent cases, since the position and the velocity curves show basically the same relative performance.) The results are also qualitatively the same in Fig 8, which is the Sensor 1 case again except the measurement update rate is one measurement every four seconds instead of every quarter of a second. The conclusion from these cases is that the three filters behave similarly for a variety of geometries and measurement update rates.

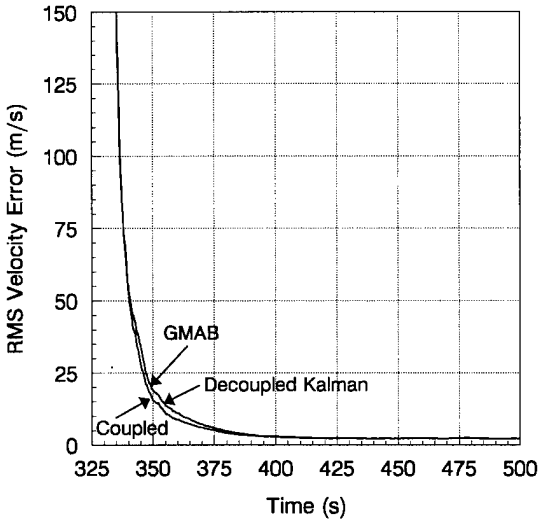

Figure 7. Velocity Errors for GMAB and Kalman Filters at Sensor Position 2.

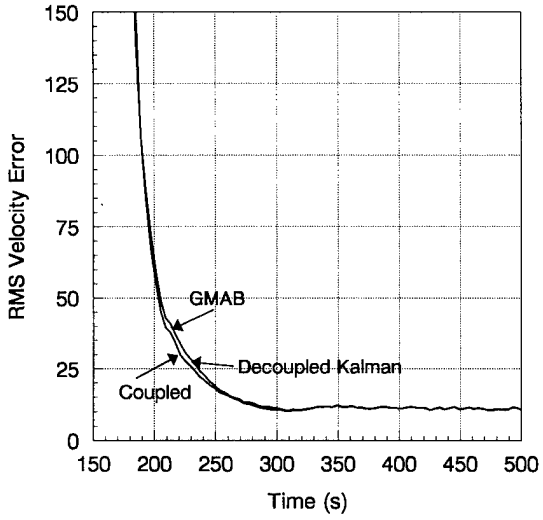

Figure 8. Velocity Errors for GMAB and Kalman Filters at Sensor Position 1, with 4 seconds between measurements.

These cases were all run with a constant measurement rate. Consider now the case when there are data loss periods. These could occur for a variety of reasons. First, the ballistic object could have a radar cross section which is changing in time due to changing angular orientation relative to the line-of-sight vector, so that the target could be fading in and out of track. In this case, the data loss periods are short enough that there is a high probability of reacquiring the target within one beam-width of the predicted target position based on the estimated state from the last measurement. A logical strategy for ballistic targets, since their dynamics are well known (assuming no thrusting periods which would effect orbit changes), is to continue to attempt to reacquire the target until the probability that the target is within one beam width is low.

The second class of causes for data loss would be intentional on the part of the sensor operator. For example, with a phased array radar, operational considerations could cause other targets to be of such a high priority that no looks at the target of interest would be scheduled for some period of time. Whatever the cause, data-loss periods are a real consideration for real ballistic missile tracking considerations.

Fig. 9 depicts what happens when one blackout period of 50 second duration occurs after the filters have settled significantly, starting at time 250 seconds. Notice the flat velocity curves between 250 and 300 seconds, due to lack of measurements. Again, the filters behave very similarly.

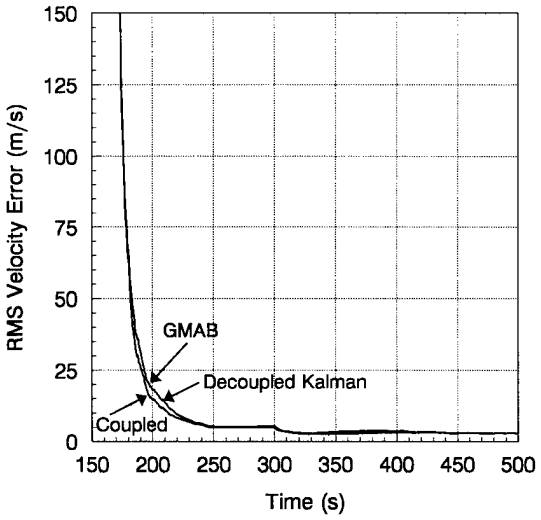

Figure 9. Velocity Errors for One Data Loss Period, After Settling.

When the target fades in and out, however, with the data losses occurring early and frequently, a different story emerges. Consider again the original Sensor 1 case, except that fading in and out of data occurs, starting 5 seconds after detection for a 20 second duration, followed by subsequent periods of 20 seconds of data, then 20 seconds of loss, and so on, until the

end of the trajectory. The results are depicted in Fig.s 10 and 11. In this case, the GMAB filter has significantly degraded performance relative to the Kalman filters.

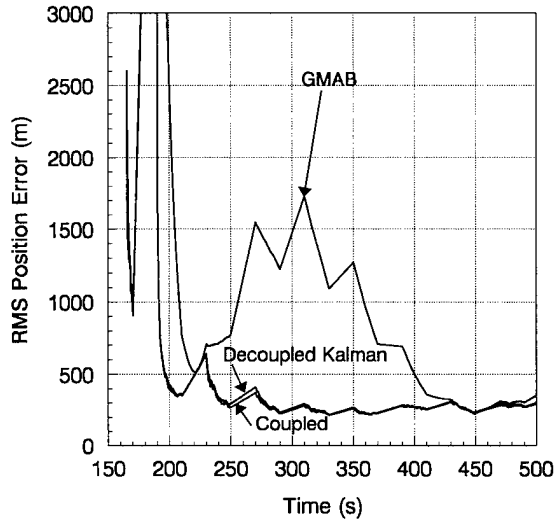

Figure 10. Position Errors for Frequent Data Loss.

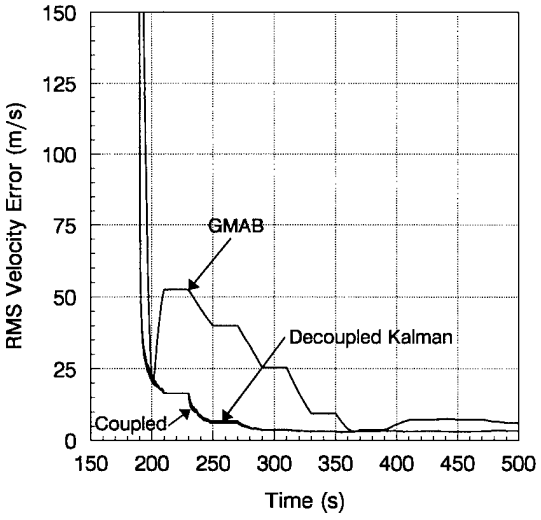

Figure 11. Velocity Errors for Frequent Data Loss.

Conclusions

Four different filtering options have been considered for the problem of tracking an exoatmospheric ballistic target with range and angle measurements. All four filters, when properly designed and tuned, are able to track the target with some degree of accuracy. The pure, constant-gain alpha-beta filter does lag significantly the other three filters in being able to simultaneously drop the errors rapidly and to settle to a low error value. An augmented alpha-beta concept, the second filtering option considered, performs about the same as the coupled extended Kalman filter, for all typical scenarios. When data-loss periods are introduced, however, its performance is degraded appreciably compared to the two Kalman filter designs.

Perhaps the most surprising of all is that the decoupled Kalman filter performs very competitively with the fully coupled extended Kalman filter, for all of the different scenarios examined. Its computational complexity is even competitive with a pure alpha-beta filter (if the alpha-beta gains are generated in real time as opposed to via a table-lookup), while it has at least an order of magnitude less complexity than the coupled Kalman filter.

References

[1]Kalman, R. E., "A New Approach to Linear Filtering and Prediction Problems," *Trans. ASME, J. Basic Engineering*, March, 1960, pp. 34-45.

[2]Kalman, R. E., and Bucy, R., "New Results in Linear Filtering and Prediction Theory," *Trans. ASME, J. Basic Engineering*, March, 1961, pp. 95-108.

[3]Morrison, N., *Introduction to Sequential Smoothing and Prediction*, McGraw-Hill, New York, 1969.

[4]Kalata, P. R., "The Tracking Index: A Generalized Parameter for Alpha-Beta-Gamma Target Trackers," *IEEE TRAns. Aerospace and Electronic Systems*, March, 1984, pp. 174-182.

[5]Bar-Shalom, Y., and Li, X.-R., "The Alpha-Beta Filter for Piecewise Constant Acceleration Model," *Estimation and Tracking: Principles, Techniques, and Software*, Artech House, Norwood, MA, 1993, pp. 275-281.

[6]Bar-Shalom, Y., and Li, X.-R., "Explicit Filters for Noiseless Kinematic Models," *Estimation and Tracking: Principles, Techniques, and Software*, Artech House, Norwood, MA, 1993, pp. 270-271.

[7]Bar-Shalom, Y., and Li, X.-R., "Direct Discrete Time Kinematic Models," *Estimation and Tracking: Principles, Techniques, and Software*, Artech House, Norwood, MA, 1993, pp. 266-269.

[8]Bate, R. R., Mueller, D. D., and White, J. E., "Position and Velocity as a Function of Time," *Fundamentals of Astrodynamics*, Dover, New York, 1971, pp. 177-226.

[9]Minter, C. F., and Lawton, J. A., "Comparison of Kalman Filter Initialization Methods," NSWCDD/TR-97/150, 1997.